1

Thermally-Formed Oxide on Magnesium and Magnesium Alloys

Teng-Shih, SHIH, Jyun-Bo LIU and Pai-Sheng WEI
National Central University (Department of Mechanical Engineering)
Taiwan (R.O.C)

1. Introduction

Magnesium alloys are commonly used in making automobile parts or by the communication industry due to their unique properties, such as low density, good damping capacity and ease of manufacturing. Magnesium alloys are very active and often cause fire hazards or surface degradation during the manufacturing processes, such as machining, melting or heat treatment. Understanding the combustion characteristics of different Mg alloys is necessary and of industrial interest.

Shih *et al.* (2002) studied the combustion of AZ61A alloys in different gases. They outlined possible reactions between Mg and O_2, CO_2 and CO based on their observations. Decreasing CO_2/Ar decreases the amount of heat derived from the oxidation reaction. Shih et al. also used a modified type of thermal analysis to study the combustion of magnesium alloyed with calcium or aluminum (Shih et al., 2004). A Mg-5Ca alloy cake was ignition-proof up to1000 K, while the solution-treated AZ91D alloy cake could also remain ignition-proof up to 1000 K during heating. The CaO oxide layer was dense so served to provide good thermal stability for the Mg-5Ca alloy. The oxide layer that formed on the surface of the solution-treated AZ91D was mainly composed of $MgAl_2O_4$ spinels, and it was this which improved the thermal stability of the solution-treated AZ91D.

Czerwinski (2002) studied the oxidation of AZ91D alloys via TGA test results. Samples were heated from 470 to 800 K. The oxidation process could be divided into three different periods: the protective layer, incubation and non-protective periods. The protective behavior was not discussed but the non-protective behavior was associated with the formation of oxide nodules and their coalescence into a loose fine-grained structure.

Zeng *et al.* (2001) studied the Auger depth profiles of AZB91 (Mg-9Al-0.5Zn-0.3Be) alloys heated at 923 and 1043 K for 10 s. For the AZ91 alloy with added Be, MgO should form prior to BeO at 923 K due to a high mole concentration ratio of Mg to Be. Beryllium possesses a lower density than magnesium (1.65 g/ml versus 1.74 g/ml) and tends to enrich its concentration beneath the top oxide layer (MgO). If the beryllium concentration is higher than 2.3 at%, BeO would form and become attached to the upper layer (or subsurface) decreasing the Be concentration in the nearby melt, where the Al concentration would gradually increase. Spinel possesses a lower free energy than BeO (−1878.75 kJ/mol versus −511.08 kJ/mol). This means that the inner layer is composed of complex oxides of MgO, BeO and spinel. The BeO possesses a low thermal expansion coefficient (17.8×10^{-6} at 298 K and 31.7×10^{-6} K^{-1} at 1000 K) compared with that of MgO (44.3×10^{-6} K^{-1} from 993 to 1933

K) (Fei In *et al.*, 1995). Consequently, the duplex oxide of BeO and spinel existing in the inner layer enhances the thermal stability of the oxide film and thus reduce the possibility of microcracks formation. Houska showed that adding 0.001 wt.% of Beryllium could delay the combustion of Mg by about 200 K (Houska, 1988). Foerster (1998) found that adding 3–8 ppm Beryllium could greatly improve the oxidation resistance of the Mg alloy. Czerwinski (2004) used TGA to study the oxidation and evaporation behavior of AZ91D magnesium alloys with 5 and 10 ppm of beryllium at temperatures between 473 and 773 K. He found that the addition of beryllium delayed the transformation from protective to non-protective behavior. In addition, in an inert atmosphere, increasing the beryllium content reduced the magnesium evaporation rate.
In this study, we discuss the morphology of a thermally formed Mg oxide layer using TGA analysis and SEM observation. We then address the protective behavior of SF_6 during the heating and melting of pure Mg. The oxide films grew on AZ91 melt and heated AZ80 cake was compared and discussed.

2. Experimental procedure

Samples of pure Mg (99.9 wt.%) in size 5 mm × 5 mm × 10 mm were prepared. Each sample was polished by p400–2000 abrasive papers without lubricants to minimize the effect of amorphous oxide formation. The samples were then promptly removed to a muffle furnace and heated under different atmospheres at 700 K for two time spans of 1 and 25 h, respectively. For growing thermal oxides on the pure magnesium sample, air mixed with and without 2% SF_6 was used as the surrounding protective atmospheres. The heated pure Mg samples grew thermal oxides on their surfaces during heating. After being cooled to room temperature, the samples were sectioned and polished and to SEM and optical observations.
A Perkin-Elmer (TGA-7) apparatus was utilized to record the thermogravimetric analysis of the pure magnesium 5 mm × 5 mm × 5 mm specimens. The weight change when the sample was heated in an air atmosphere with a flow rate of 50 cm^3/min was measured. The specimen was preheated up to 423 K at a heating rate of 10 K/min, then held for a period of 1800 s. It was then heated to the reaction temperature of 700 K at a heating rate of 10 K/min and held for 2.16×10^4 s.
Electron Spectroscopy for Chemical Analysis (ESCA, Thermo VG Scientific Sigma Probe) was used to analyze the composition of the surface oxides. The relationship of the composition-depth profiles was obtained by using a 3 keV argon ion beam at 0.1 cm^{-2}. The chemical composition of the thermally formed oxide layer was also checked by using an Electron Probe Micro Analyzer (EPMA, Joel JXA-8600SX). Experimental data for AZ91, from the work of (Zeng *et al.,* 2001), are also discussed.

3. Results and discussion

3.1 Thermogravimetric analysis at pure magnesium

The results of the thermogravimetric analysis of pure magnesium are recorded in Fig. 1. The data show a weight gain during the short time when the cubic sample was preheated at 423 K for 1800 s in an air atmosphere. When magnesium was heated in air, it became hydrated (>120 °C) to form brucite ($Mg(OH)_2$). However, brucite dehydrayion is reversible (brucite = periclase + water); this reaction can be shifted in either direction by increasing or decreasing

the water vapor pressure at the appropriate temperature (Sharma *et al*., 2004) and (Schramke *et al*., 1982). The weight change then decreased rapidly due to the dehydroxylation of brucite. The sample's weight stabilized when the temperature reached 700 K; see stage III in Fig. 1. After this stable period (or protective behavior), the weight again increased rapidly in stage IV, as shown in Fig. 1. When pure magnesium is placed in contact with oxygen, the following reactions occur: first, oxygen chemisorption on the surface of the magnesium, then the formation and coalescence of oxide islands, and finally oxide thickening. When there is water vapor, the reaction leads to the formation and growth of an oxide layer, but the reaction rate is much less than in an oxygen atmosphere, and the oxide layer will contain relatively large amounts of hydroxyl or hydroxide species (Splinter *et al*., 1993) and (Fuggle *et al*., 1975). The Gibbs free energy of brucite and periclase are −711.8 and −525.8 kJ/mol at 700 K, respectively (Robie *et al*., 1978). When a pure magnesium sample is heated in an air atmosphere, brucite forms first, especially at low-temperatures. Brucite is then transformed to periclase by the dehydration or dehydroxylation associated with a large decrease in volume (~50%) during the reaction process (Sharma *et al*., 2004).

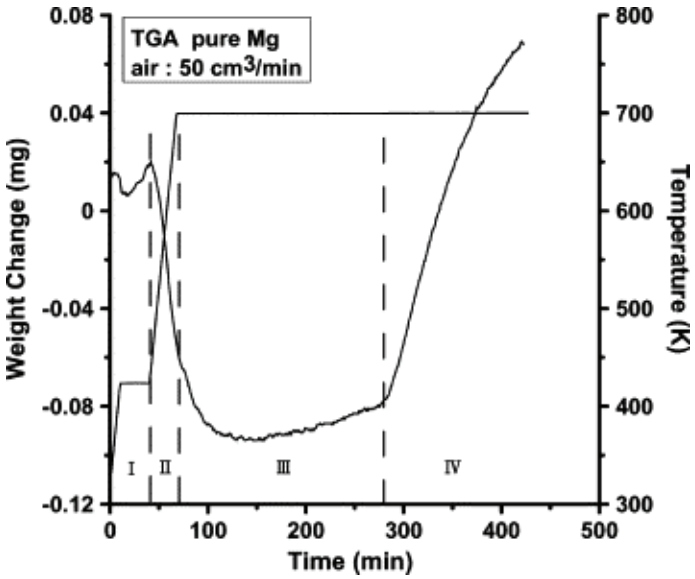

Fig. 1. Thermogravimetric analysis of pure magnesium (99.96 wt.%); heating rate $\partial T/\partial \tau$ = 10 ^{o}C min^{-1}; air flowing rate = 50 cm^3/min.

The protective behavior occurs during stage III (Fig. 1) due to a lack of easy paths for fast Mg transport (Shih *et al*., 2006). Fig. 2a and b shows the sectional morphologies of a sample heated at 700 K for 3.6 × 10^3 s. The protective behavior for this holding time is shown by the thermogravimetric analysis; Fig. 1. Microchannels and microcracks are visible, but these channels or cracks do not penetrate through the oxide film; meaning, there are no easy path for magnesium transport. Brucite dehydrated and formed lamella MgO during heating. Concurrently, dehydroxylation also brought water vapor to the surface of the brucite film. Crystalline MgO can be rehyroxylated by increasing the water vapor pressure (Schramke *et al*., 1982). During heating, dehydroxylation is energetically favorable for transforming

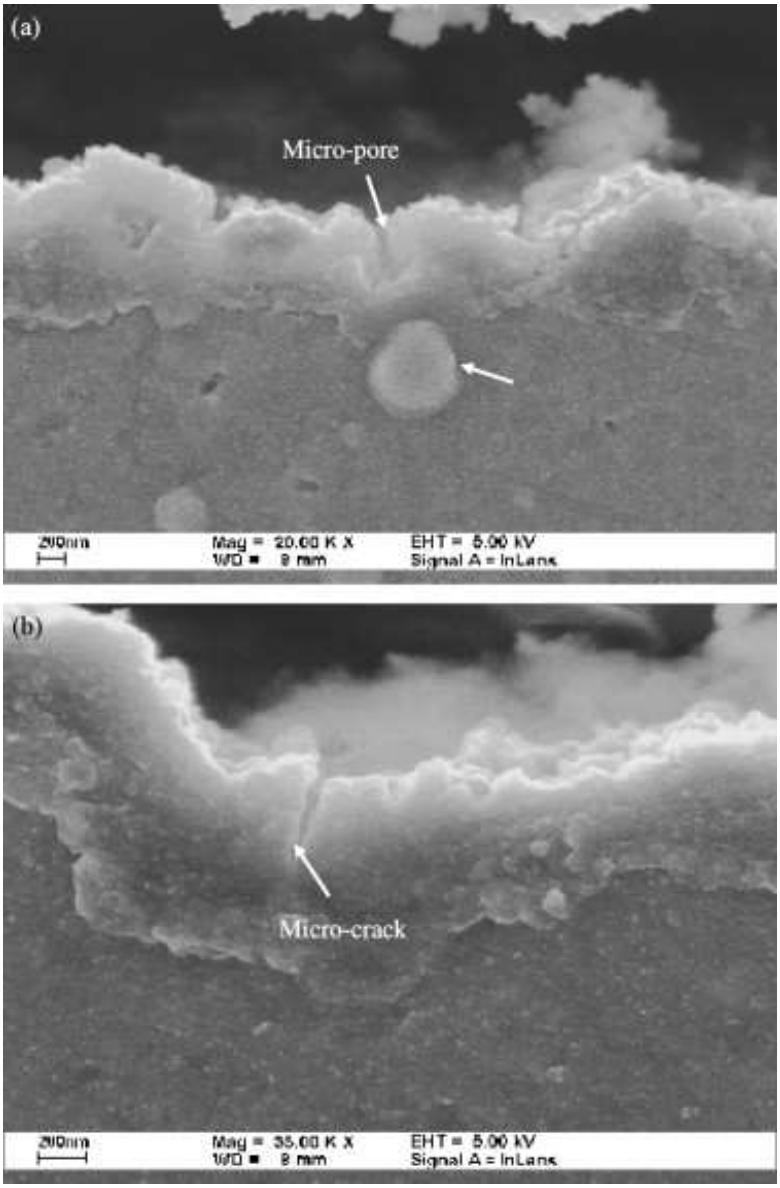

Fig. 2. SEM photos showing the sectional view including oxide film and substrate; sample (99.956 wt.% Mg) heated at 700 K for 1 h after being polished by abrasive paper; (a) magnification 20,000× and (b) magnification 35,000×.

brucite into MgO. Rehydroxylation may also occur locally at points which a high vapor pressure exists. Nanoscale cracking and fragmentation occur during dehydroxylation (Sharma *et al.*, 2004). Then, magnesium containing species could fill the cracks due to high mobility during heating. They react with the steam vapor to form brucite, which heals the microcracks. In our experiments, the fresh brucite on the microcrack walls and valley is transformed into periclase due to dehydroxylation at 700 K. The above reactions proceeded periodically during heating causing a protective behavior in stage III; see Fig. 1. When most of the brucite was transformed to MgO, the water vapor was almost completely depleted. The great difference in thermal expansion coefficient between magnesium and MgO caused the oxide film to crack. These cracks acted as channels for transporting magnesium vapor outward to react with the oxygen, result in the formation of ridges and/or nodules associated with a rapid weight gain (a non-protective behavior) in stage IV of Fig. 1.

Fig. 2a shows an inclusion particle located underneath the oxide film and a microchannel that is pointing to but not open to the particle. The thickness of the oxide layer varied from 0.6 to 1 μm and the microcracks were open for about half the thickness of the layer. This microcrack formation may have been triggered by the particles so that dehyroxylation and rehydroxylation could persist for a longer period of time.

Non-protective behavior occurs when the rehydroxylation process terminates and all the oxide has become periclase. Open microcracks allow the transportation of Mg to react with

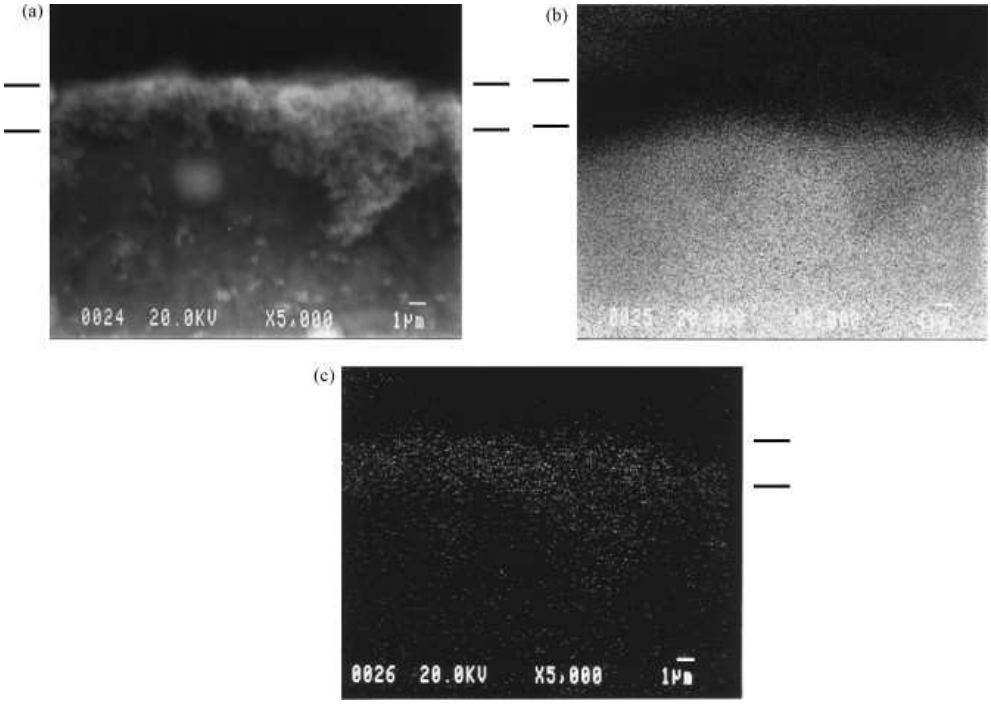

Fig. 3. EPMA photos showing the sectional view including oxide film and substrate; sample (99.956 wt.% Mg) heated in air at 700 K for 25 h, sample polished by abrasive papers; (a) magnification 5000×; (b) Mg mapping and (c) O mapping.

the oxygen to form periclase. Fig. 3 shows the oxide penetration into the pure Mg substrate. Ridges formed after the sample was heated in air at 700 K for 9×10^4 s. Extending the heating time or raising the temperature causes the reaction to become much more rigorous, forming more nodules on the oxide film, leading to a loose structure, as illustrated by Czerwinski (2004).

3.2 The effect of SF_6 on the oxide film on pure magnesium

During the melting of magnesium alloys, CO_2, SO_2 and SF_6 gases are often used as the protective atmospheres. Using SF_6 can efficiently prevent magnesium ignition, but it also has a significant negative impact due to the greenhouse effect. A better understanding of the reaction of Mg with SF_6 is thus of industrial interest.

Samples of pure Mg were heated at 700 K for 9×10^4 s in an atmosphere of air mixed with 2% SF_6. The samples were sectioned, polished and then observed by SEM and analyzed by an Electron Probe Micro Analyzer. Fig. 4b–d shows the Al, F and S mapping, respectively. The tested fluorine resided at the interface between the substrate and the thermally formed oxide layer. Sulfur was incorporated with the fluorine near the oxide layer, but its intensity was far less than that of the fluorine. Aluminum showed locally at the substrate and oxide layer interface indicating the possibility of the existence of spinels.

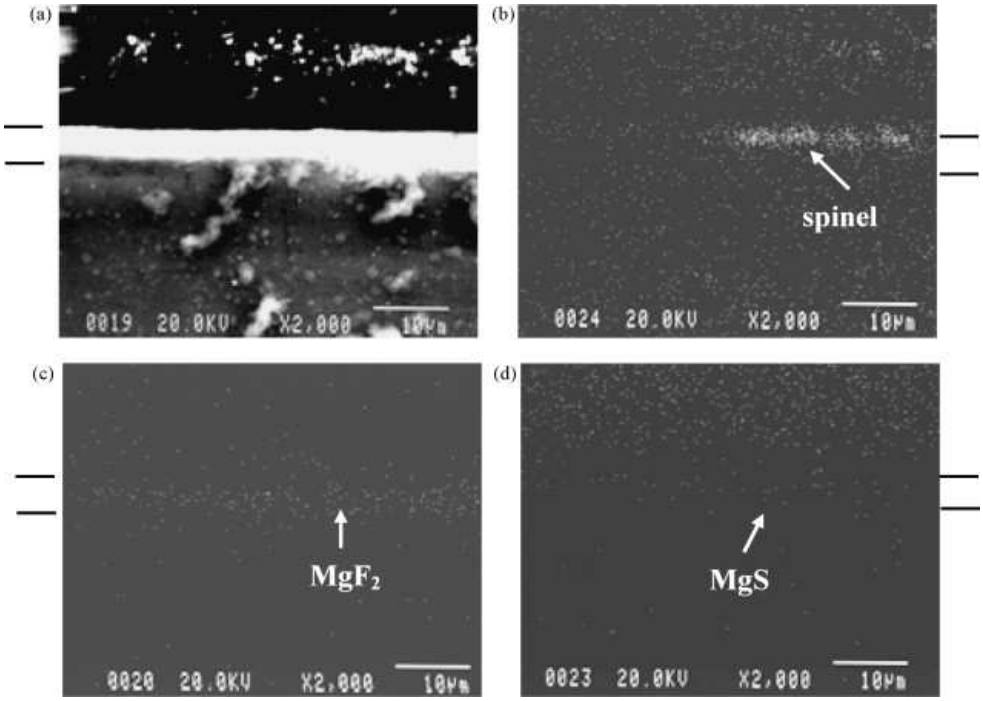

Fig. 4. EPMA photos showing the sectional view including oxide film and substrate; sample (99.956 wt.% Mg) heated in a protective atmosphere (0.2% SF_6) at 700 K for 25 h; sample polished by abrasive papers; (a) magnification 2000×; (b) Al mapping; (c) F mapping and (d) S mapping.

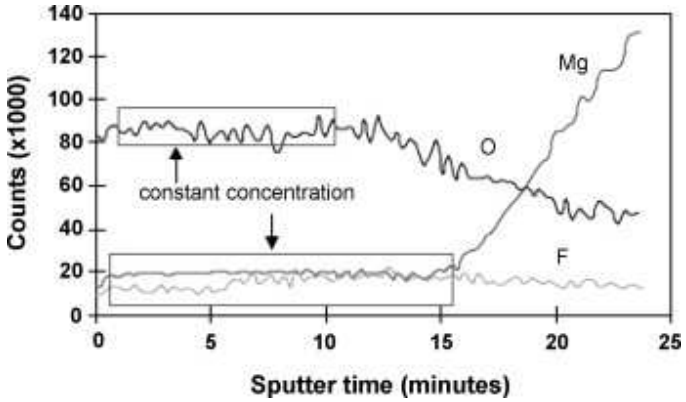

Fig. 5. The square of the film thickness versus film exposure time, for film samples produced under a cover gas of air containing 0.3% at 973 K

As explained previously, brucite formed during heating. It turned out to become periclase when dehydroxylation occurred. At a high-temperature (700 K), magnesium containing species diffused out from the substrate via the microcracks to react with oxygen to form periclase and also released latent heat (ΔH = 600.5 kJ/mol). The protective atmosphere contained a small fraction of SF_6 (about 2%) which is heavier than CO_2 and air (6.4 kg dm^{-3} for SF_6, 1.9 × 10^{-3} kg dm^{-3} for CO_2, and 1.2 × 10^{-3} kg dm^{-3} for air). The SF_6 might fill up the microcracks in the thermally formed oxide layer and was heated by the reacting periclase. SF_6 can be decomposed if sufficient heat is available: ΔH = −1221.6 kJ/mol. In other words, a reaction of two moles of MgO can offer enough latent heat to decompose one mole of SF_6. The SF_6 was heated and reacted with Mg to form MgF_2 (formation enthalpy −1120.1 kJ/mol; formation energy −1001.2 kJ/mol (Barin, 1995)). The above reactions occurred persistently; forming periclase, decomposing SF_6, and then producing MgF_2. The MgF_2 was incubated in the microcracks and gradually filled the interface between the magnesium substrate and the oxide layer.

In this study, we used an atmosphere of air mixed with 2% SF_6. It is reasonable to postulate that MgF_2 and MgS coexisted at the interfacial layer between the oxide and the substrate, as indicated by the F and S mapping. Aluminum is soluble in magnesium and would thus diffuse out to form spinel during heating since the formation energy is −2005.6 kJ/mol at 700 K, which is more favorable than MgF_2 (−1001.2 kJ/mol) or MgO (−525.8 kJ/mol). When the Mg sample was heated and held at 700 K in an atmosphere of air mixed with 2% SF_6, spinel could form at the interfacial layer between the oxide and the substrate, where MgF_2 formed on the surface of the substrate. MgF_2 possesses a cubic structure similar to TiO_2 and has a low thermal expansion coefficient of 18 × 10^{-6} K^{-1} (a_a) and 13.7 × 10^{-6} K^{-1} (a_c), compared with MgO which is 44.3 ×10^{-6} K^{-1} (Fei In et al., 1995) and (Krishna Rao *et al.*, 1962). The MgF_2 film can therefore provide protection to the magnesium during heating.

Cashion *et al* (2002). prepared a film sample by melting Mg in a covering gas of air containing 0.3% SF_6 at 973 K. The film was about 0.25 μm in thickness after an exposure time of 1 h. In this study, the thermally formed oxide layer was about 6–8 μm, as indicated in Fig. 4, after magnesium was heated at 700 K in air containing 2% SF_6. The thickness of the thermally formed oxide film was far greater than that of the film deposed on the melt, although the former was heated at 700 K and the latter was treated at 973 K.

The Auger electron spectroscopy tests show the relation of the film composition versus sputtering time; see Fig. 5 (Cashion *et al.*,2002a). Fluorine can be detected. The MgF_2 product showed from the interfacial layer between the oxide film and the substrate was about one-half the thickness of the film. In this study, the MgF_2 occupies less than one half of the territory of the thermally formed oxide film (which was formed at 700 K for 1 h under a covering gas containing 2% SF_6); see Fig. 4. Two important observations can be made after comparing Fig. 4 and Fig. 5. First, MgF_2 was apparently preferentially located at the interfacial layer between the oxide film and the Mg substrate. Second, increasing the heating temperature increased the MgF_2 in the oxide film was evident experimentally.
During the heating thermally formed oxides first formed brucite which was then transformed to periclase at a high-temperature. Microcracks formed and the magnesium containing species diffused outward to react with the oxygen. The MgO would cover the surface of the heated Mg whether in the solid or in the melt. The reacting MgO product released heat, decomposing SF_6, resulting in the formation of MgF_2. Magnesium diffused out from the substrate via microcracks. Therefore, the MgF_2 product was preferentially located in the microcrack valleys. Increasing the heating temperature increased the reaction rate for forming MgO, offering a higher driving force for decomposing SF_6 and forming MgF_2 at the microcrack valleys. Therefore, MgF_2 was deposited underneath the MgO, and grew from the interfacial layer. The thickness of the MgF_2 layer increased following an increase in temperature and/or heating time. It therefore occupied a greater fraction of the oxide film and provided protection for the Mg melt as is the case in Fig. 5 (film on the melt) and in Fig. 4 (thermally formed film).
Spinel ($MgAl_2O_4$) is more energetically favorable at 700 K (−2005.6 kJ/mol) than either AlF_3 (−1326.2 kJ/mol) or MgF_2 (−1001.2 kJ/mol). It preferentially forms at areas where aluminum has diffused out from the Mg matrix and reacted with oxygen. The reacting spinel releases latent heat (−2297.8 kJ/mol) which generates a great driving force for decomposing SF_6. Fluorine mapping thus shows the obvious intensity nearby the colony, corresponding to the Al mapping in Fig. 4.

3.3 Oxidation of AZ80 heated in air

The solution-treated AZ80 alloy sample was heated in air at 700K up to 1h. The surface of the heated sample changed in color from a bright metallic to a matt gray, reflecting the existence of the oxide film. Optical observation indicated that there were some small nodules distributed over the surface. Fig. 6a and b shows sectional views of the sample observed by SEM. Microcracks resided within the thermally formed oxide film. The crack sizes were less than those found within the thermally formed oxide film from the pure Mg sample; Fig. 2a and b. These microcracks can act as an easy path allowing the diffusion of Mg, to react with the oxygen, which produced the nodular structure.
The ESCA analysis shows the concentration-depth profile of the solution-treated AZ80 sample; see Fig. 7. The outer layer is mainly MgO. The concentration profiles of magnesium, oxygen and aluminum show a plateau on the intermediate region. This region is mostly composed of MgO and some spinel ($MgAl_2O_4$). The latter phase increased with the depth of oxide film in conjunction with the increase in the aluminum content. The spinel fraction increased up to a point where the oxygen content became level after dropping. The atomic percentage of oxygen and magnesium in the spinel was about 57.1 and 14.3%, respectively. Spinel formation would consume a large amount of oxygen. The oxygen diffused inward from the surrounding atmosphere. Increasing the oxide film thickness increased the difficulty for oxygen diffusion, limiting the spinel reaction to some extent, as shown in Fig. 7.

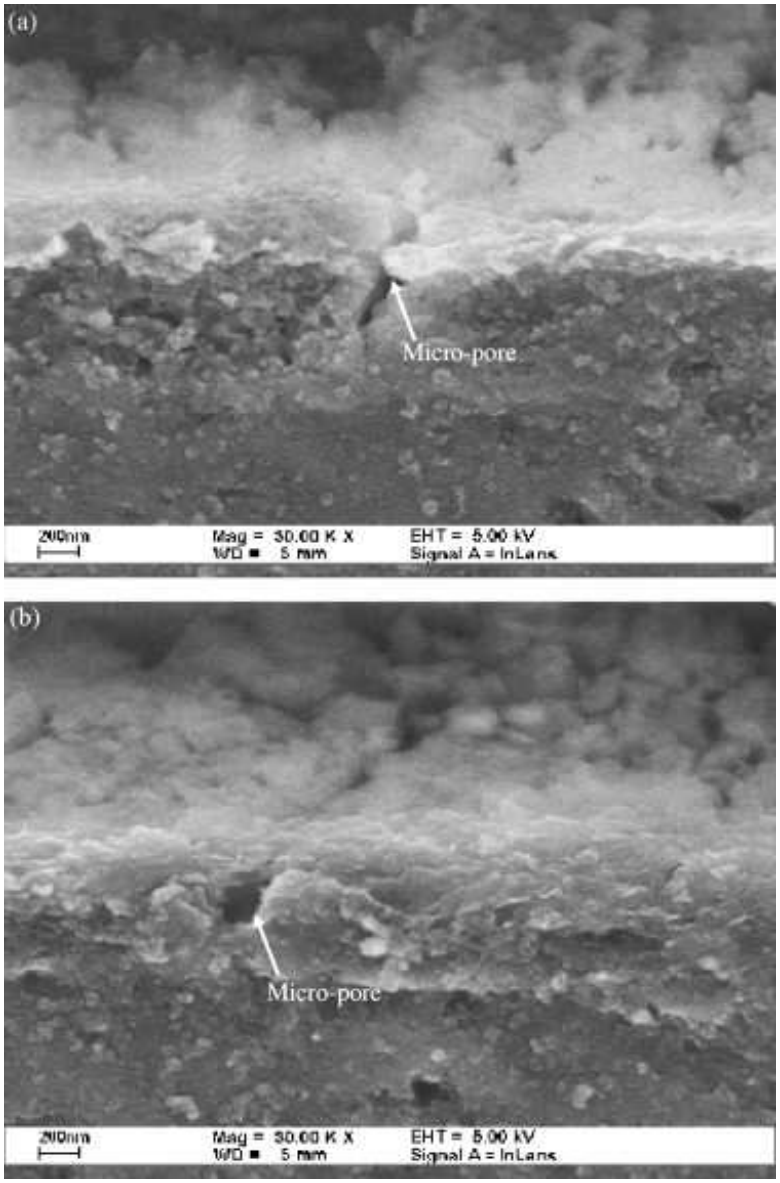

Fig. 6. SEM photo shows the sectional view of solution-treated AZ80 sample after polish by abrasive papers and heated in air at 700 K for 1 h; (a) and (b) magnification 30,000× showing the existence of micropore.

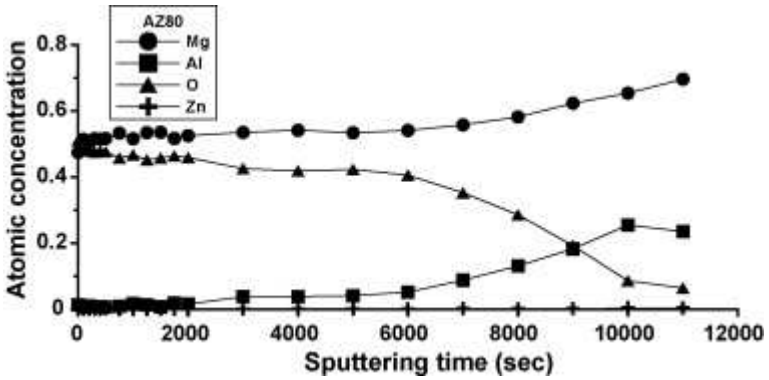

Fig. 7. ESCA analyses showing the measured atomic concentrations of Mg, O, Al and Zn versus sputtering time on solution-treated AZ80 after polished by abrasive papers and heated at 700 K for 1 h; the total sputtering time 11000 s.

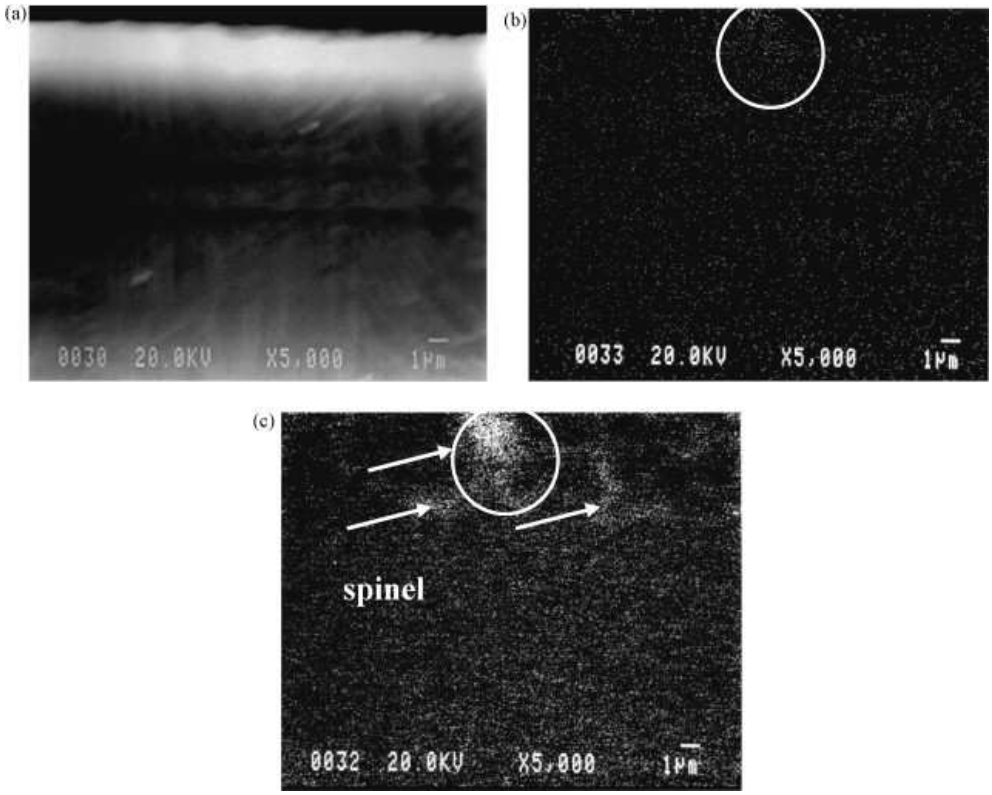

Fig. 8. EPMA photos showing the sectional view including oxide film and substrate; solution-treated AZ80 heated in air at 700 K for 1 h; sample polished by abrasive papers; (a) magnification 5000×; (b) O mapping and (c) Al mapping.

Fig. 8 shows the EPMA analyses of oxygen and aluminum. From the coexistence of Al, O and Mg, it can be reasonably postulated that this area is composed of spinel. This is distributed near the interfacial layer, but is more like a network in the oxide film. The formation energies of spinel and periclease are −1878.75 and −493.09 kJ/mol (at 1000 K), respectively. After being heated, MgO will form on the sample surface first after which aluminum concentration in the substrate increases. This is energetically favorable for formation spinel. The thermal expansion coefficient of spinels, 29.4×10^{-6} K^{-1}, is far less than that of MgO, 44.3×10^{-6} K^{-1}, at a heating temperature of 1000 K (Fei In *et al.*, 1995). Spinel is much more thermally stable than MgO. This means that the solution-treated AZ80A could resist ignition up to 823 K (Shih *et al.*, 2004).

3.4 Oxidation films on the AZ91 melt and AZ80 heated cake

In the reference work of Zeng et al., an AZ91 (Mg-9Al-0.5Zn) alloy was prepared using commercially pure Mg, Al, and Zn. The alloy was melted in an electric resistance furnace. When the melt temperature reached 973 K, the oxide film was removed from the melt. The melt was then poured into a permanent mold to obtain cakes with a diameter of 80 and 70 mm in thickness. The cakes were remelted in a crucible at 923 K for 10 s to prepare the surface oxide samples.

ESCA analyses were done to show the concentration-depth profiles of the elements on the oxide film; see Fig. 9a. The surface layer is rich in magnesium; the ratio of magnesium to oxygen is greater than 1. The oxygen content remains constant for a short distance then gradually decreases with depth. Periclase is the main constituent phase in this layer with some magnesium trapped in the MgO making the magnesium to oxygen ratio greater than 1. The magnesium concentration drops when there is a significant increase in the aluminum concentration indicating the existence of spinel in this region, Fig. 9b.

Comparing Fig. 7 and Fig. 9, we can make the following conclusions: (1) the thickness of the oxide film developed from the AZ91 melt is about 0.5–0.6 μm and the thermally formed oxide film deposited on the solution-treated AZ80 is about 4–6 μm. The former sample was melted at 923 K for 10 s and the latter was heated at 700 K for 3600 s. In other words, the reaction time is the influential factor in determining the thickness of the oxide film; (2) the concentrations of Mg, Al and O versus depth profiles of both the AZ 91 and AZ80 samples show a similar pattern and (3) the oxide film developed from the AZ91 melt possesses a higher magnesium concentration in the top layer than that obtained from the heated AZ80. The former oxide film contains more than 50% magnesium and the latter about 50% Mg. This difference was caused by the heating temperature (Fig. 10).

Fig. 9b schematically illustrates the prospective phases contained in the oxide film on the AZ91 sample. The top layer (zone I) is rich in MgO, with some Mg trapped in the microcracks. The intermediate layer (zone II) is composed of spinel, MgO and trapped Mg. In this layer, the spinel comprises a high fraction in the region close to the inner layer (zone III) but MgO is dense in the region close to the outer layer (zone I). The MgO and spinel have decreased fractions in the inner layer, but Mg greatly increases in concentration approaching the substrate.

During heating, brucite is transformed to periclase by the incorporation of voids and microcracks. Magnesium diffuses from the microcracks to react with oxygen, increasing the thickness of the periclase in conjunction with the magnesium trapped in the oxide layer. When perilcase increases in thickness to some extent, the microcracks will again open, and

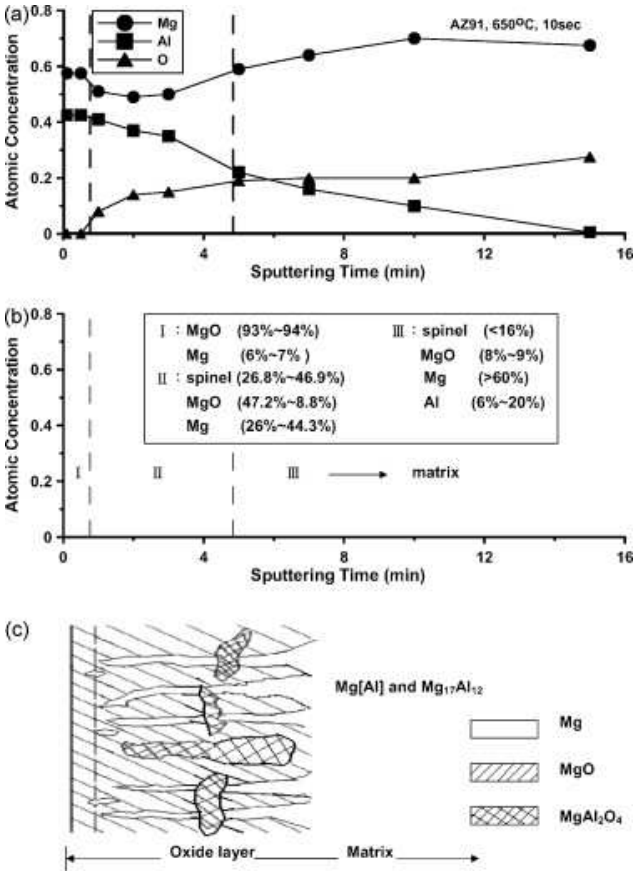

Fig. 9. (a) Relationship of Al, O and Mg concentrations versus sputtering time for sample of AZ91 alloy melted at 923 K for 10 s (Zeng *et al*., 2001); (b) the prospective phases along with the estimated fractions of each oxide resided at different zones in the oxide film and (c) schematically illustrated the different oxide and trapped Mg in the oxide film.

newly formed periclase erupts into the melt forming a new layer of oxides. This process persists, increasing the thickness of the oxide film and also allowing for chance to form spinels. There are two possible paths for spinel formation: (1) metastable MgO can react with the Al–Mg melt to form spinel by $4MgO + 2Al \Rightarrow MgAl_2O_4 + 3Mg$ (Salas *et al*., 1991) and (2) the oxide film fractures generating a chance for the reaction of oxygen with the Mg–Al melt. Aluminum has a higher density than Mg (2.7 g/cm^3 versus 1.74 g/cm^3) so after the top surface layer of the MgO increases in thickness, the Al content in the subsurface of the melt tends to increase. Spinel formed via this reaction (path (1)) is likely to be located at the oxide film and substrate interface but that formed via the microcrack, path (2), would more likely be located within the oxide film; see Fig. 8b. Once the spinel fraction in the oxide film increased the thermal stability of the oxide film improved blocking the microchannels transporting metal from the melt (Cashion *et al*., 2002b). Fig. 9c schematically illustrates the distribution of MgO, spinel and Mg trapped in the oxide film.

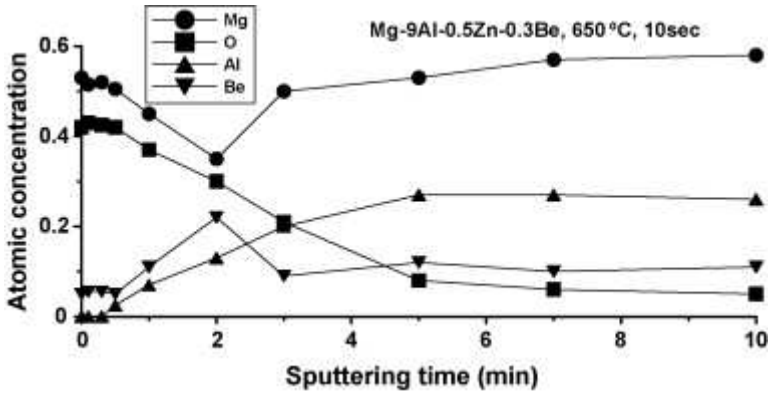

Fig. 10. Relation of Al, O, Mg and Be concentrations versus sputtering time for sample of AZB91 alloy melted at 923 K for 10 s

4. Conclusion

The ignition-proofing of a magnesium alloy can be obtained by using an inert gas atmosphere and/or by an alloying procedure. Magnesium alloys can usually be protected by CO_2, SO_2 or SF_6 using an inert gas atmosphere. There are many elements of the alloying procedure that have already been studied, including calcium, aluminum and so on. Based on the present studies, the following conclusions can be made:

(1) Brucite forms on magnesium and is transformed into periclase by the dehydration process. Microcracks caused by the large volume change of dehydration provide an easy path for evaporating Mg. Each path can produce a nodule on the surface of the oxide film. For an oxide film with a high population of nodules, the reacting MgO will ignite the melt or the heated alloy.

(2) When inert gas SF_6 was used, MgF_2 or MgS, can form on the surface of pure magnesium at the interfacial layer between the oxide and the substrate where the reacting MgF_2 could block the diffusion of Mg from the substrate.

(3) As a result of adding element Al, a trace of spinel was observed in the magnesium oxide layer. The reacting spinel tended to form at the interfacial layer which affected Mg diffusion from the substrate, improving the ignition-proofing of heated sample.

(Paper had originally published in Materials Chemistry and Physics 104 (2007))

5. Reference

Shih, T. S., Chung, C. B. and Chong, K. Z. (2002). *Mater. Chem. Phys.* 74, 66.

Shih, T. S., Wang, J.H., and Chong, K. Z. (2004). *Mater. Chem. Phys.* 85, 302.

Czerwinski, F. (2002). *Acta Mater.* 50 2639.

Zeng, X. Q., Wang, Q. D., Lu, Y. Z., Ding, W. J., Zhu, Y. P., Zhai, C. Q., Lu, C. and Xu, X. P. (2001). *Mater. Sci. Eng. A Struct. Mater.: Prop. Microstruct. Process.* 301, 154.

Fei In, Y. (1995), *"Mineral Physics and Crystallography: a Handbook of Physical Constants"*, Ahrens, T. J., ISBN-0875908527, American Geophysical Union, Washington, D.C.

Houska, C. (1988). *Met. Mater.* 4, 100.
Foerster, G. (1998). *Adv. Mater. Process.* 154, 79.
Czerwinski, F. (2004). *Corros. Sci.* 46, 377.
Sharma, R. McKelvy, M. J., Bearat, H. Chizmeshya, A. V. G. and Carpenter, R. W. (2004). *Philos. Mag. A Phys. Condens. Matter Defects Mech. Prop.* 84, 2711.
Schramke, J. A., Kerrick, D. M. and Blencoe, J. G. (1982). *Am. Miner.* 67, 269.
Splinter, S. J., McIntyre, N. S., Lennard, W. N., Griffiths, K.and Palumbo, G. (1993). *Surf. Sci.* 293, 130.
Fuggle, J. C., Watson L. M. and Fabian, D. J. (1975). *Surf. Sci.* 49, 61.
Robie, R. A., Hemingway, B. S. and Fisher J. R. (1978). "*Thermodynamic Properties of Minerals and Related Substances at 298.15 K and 1 Bar Pressure and at High Temperature*", *ISBN-1*-933762-07-*1*, U.S. Geological Survey Bulletin. 1452.
Shih, T. S. and Liu, Z. B. (2006). *Mater. Trans. JIM* 47, 1347.
Barin, I. (1995), "*Thermochemical Data of Pure Substances (third ed.)*", VCH Publishers, ISBN-3527287450, New York.
Krishna Rao, K. V., Nagender Naidu, S. V. and Setty, P. L. N. (1962). *Acta Crystallogr.* 15, 528.
Cashion, S. P., Ricketts, N. J. and Hayes, P. C. (2002a). *J. Light Met.* 2, 37.
Salas, O., Ni, H., Jayaram, V., Vlach, K. C., Levi, C. G. and Mehrabian, R. (1991) *J. Mater. Res.* 6, 1964.
Cashion, S. P., Ricketts, N. J. and Hayes, P. C. (2002b) *J. Light Met.* 2, 43.

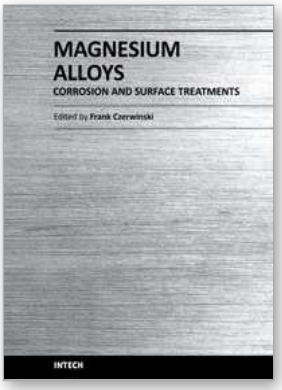

Magnesium Alloys - Corrosion and Surface Treatments
Edited by Frank Czerwinski

ISBN 978-953-307-972-1
Hard cover, 344 pages
Publisher InTech
Published online 14, January, 2011
Published in print edition January, 2011

A resistance of magnesium alloys to surface degradation is paramount for their applications in automotive, aerospace, consumer electronics and general-purpose markets. An emphasis of this book is on oxidation, corrosion and surface modifications, designed to enhance the alloy surface stability. It covers a nature of oxides grown at elevated temperatures and oxidation characteristics of selected alloys along with elements of general and electrochemical corrosion. Medical applications are considered that explore bio-compatibility of magnesium alloys. Also techniques of surface modifications, designed to improve not only corrosion resistance but also corrosion fatigue, wear and other behaviors, are described. The book represents a valuable resource for scientists and engineers from academia and industry.

INTECH
open science | open minds

InTech Europe
University Campus STeP Ri
Slavka Krautzeka 83/A
51000 Rijeka, Croatia
Phone: +385 (51) 770 447
Fax: +385 (51) 686 166
www.intechopen.com

InTech China
Unit 405, Office Block, Hotel Equatorial Shanghai
No.65, Yan An Road (West), Shanghai, 200040, China
中国上海市延安西路65号上海国际贵都大饭店办公楼405单元
Phone: +86-21-62489820
Fax: +86-21-62489821